

Article

## N-Vinyl and N-Aryl Hydroxypyridinium Ions: Charge-Activated Catalysts with Electron Withdrawing Groups

George F Riegel, and Steven Robert Kass

*J. Org. Chem.*, **Just Accepted Manuscript** • DOI: 10.1021/acs.joc.0c00498 • Publication Date (Web): 08 Apr 2020

Downloaded from [pubs.acs.org](https://pubs.acs.org) on April 16, 2020

### Just Accepted

“Just Accepted” manuscripts have been peer-reviewed and accepted for publication. They are posted online prior to technical editing, formatting for publication and author proofing. The American Chemical Society provides “Just Accepted” as a service to the research community to expedite the dissemination of scientific material as soon as possible after acceptance. “Just Accepted” manuscripts appear in full in PDF format accompanied by an HTML abstract. “Just Accepted” manuscripts have been fully peer reviewed, but should not be considered the official version of record. They are citable by the Digital Object Identifier (DOI®). “Just Accepted” is an optional service offered to authors. Therefore, the “Just Accepted” Web site may not include all articles that will be published in the journal. After a manuscript is technically edited and formatted, it will be removed from the “Just Accepted” Web site and published as an ASAP article. Note that technical editing may introduce minor changes to the manuscript text and/or graphics which could affect content, and all legal disclaimers and ethical guidelines that apply to the journal pertain. ACS cannot be held responsible for errors or consequences arising from the use of information contained in these “Just Accepted” manuscripts.

1  
2  
3  
4  
5  
6 ***N*-Vinyl and *N*-Aryl Hydroxypyridinium Ions: Charge-Activated**  
7  
8 **Catalysts with Electron Withdrawing Groups**  
9  
10

11  
12 George F. Riegel and Steven R. Kass\*

13  
14  
15  
16 Department of Chemistry, University of Minnesota  
17  
18 207 Pleasant Street, SE, Minneapolis, Minnesota 55455, United States  
19  
20

21 E-mail: [kass@umn.edu](mailto:kass@umn.edu)  
22  
23  
24  
25  
26  
27  
28  
29  
30  
31  
32  
33  
34  
35  
36  
37  
38  
39  
40  
41  
42  
43  
44  
45  
46  
47  
48  
49  
50  
51  
52  
53  
54  
55  
56  
57  
58  
59  
60

**ABSTRACT**

Charge-enhanced Brønsted acid organocatalysts with electron withdrawing substituents were synthesized and their relative acidities were characterized by computations, 1:1 binding equilibrium constants ( $K_{1:1}$ ) with a UV-vis active sensor,  $^{31}\text{P}$  NMR shifts upon coordination with triethylphosphine oxide, and in one case by IR spectroscopy. Pseudo-first order rate constants were determined for the Friedel–Crafts alkylation of *N*-methylindole with *trans*- $\beta$ -nitrostyrene and 2,2,2-trifluoroacetophenone, and the Diels–Alder reaction of cyclopentadiene with methyl vinyl ketone. These results along with kinetic isotope effect determinations revealed that the rate determining step in the Friedel–Crafts transformations can shift from carbon-carbon bond formation to proton transfer to the catalyst's conjugate base. This leads to an inverted parabolic reaction rate profile and slower reactions with more acidic catalysts in some cases. Electron withdrawing groups placed on the *N*-vinyl and *N*-aryl substituents of hydroxypyridinium ion salts lead to enhanced acidities, more acidic catalysts than trifluoroacetic acid, and a linear correlation between the logarithms of the Diels–Alder rate constants and measured  $K_{1:1}$  values.

## INTRODUCTION

Acid-catalyzed reactions are commonplace and are utilized in a wide variety of transformations spanning from the synthesis of small molecules to biocompounds and polymers. The development of Brønsted acids and hydrogen bond donating organocatalysts, consequently, is of significant interest and a subject of considerable research efforts.<sup>1,2</sup> Incorporation of electron withdrawing groups into these species not only increases their acidities and hydrogen bond donor abilities, but also typically leads to more active catalysts and enhanced reaction rates.<sup>3,4</sup> Extension of this strategy with the use of one or more positively charged centers was recently reported to be particularly effective in non-polar solvents leading to rate accelerations corresponding to orders of magnitude compared to non-charged substituents.<sup>5</sup> Even more active catalysts can be envisioned by introducing electron withdrawing groups into positively charged substrates. To explore this idea, a series of six model hydroxypyridinium salts were examined (**1–6**, Figure 1). In this report, we describe the syntheses of these six compounds, companion density functional theory computations, IR, UV-vis, and <sup>31</sup>P NMR spectroscopic studies, along with kinetic isotope effect and rate constant determinations to assess catalyst acidities, activities, and reaction mechanisms.

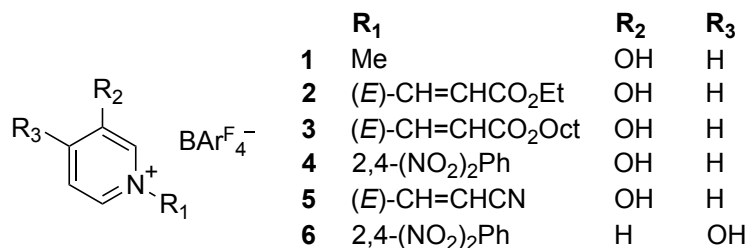


**Figure 1.** Catalysts used in this work.

## RESULTS AND DISCUSSION

The tetrakis[3,5-bis(trifluoromethyl)phenyl]borate ( $\text{BAr}^{\text{F}_4^-}$ ) salt of the *N-n*-octyl-3-hydroxypyridinium ion has previously been reported,<sup>5a</sup> and its *N*-methyl analog (**1**) was made in a similar way.<sup>5d</sup> Various strategies were employed for the preparation of the halide precursors of the other model species. Compound **2-Cl** was synthesized via a modification of the procedure from Jung and Buszek<sup>6</sup> whereas **3-Cl** was formed using an analogous method to Katrizky et al.<sup>7</sup> The preparation of **5-Br** was accomplished using a similar procedure to that of Eicher-Lorka et al.,<sup>8</sup> and the 2,4-dinitrophenyl-substituted catalyst precursors, **4-Cl** and **6-Cl**, were obtained via a similar route to the one reported by Eda, Kurth, and Nantz.<sup>9</sup> Conversions of the halide salts to their  $\text{BAr}^{\text{F}_4^-}$  analogs were carried out largely in the same way and took advantage of the differential solubilities of NaCl and NaBr compared to  $\text{NaBAr}^{\text{F}_4}$  in organic solvents.

Catalyst acidities were first evaluated at 298 K in the gas phase without the  $\text{BAr}^{\text{F}_4^-}$  counteranion using B3LYP/6-31G(d,p) computations (Table 1). This methodology was previously used to reproduce experimental Brønsted acidities and successfully predict catalyst activities in non-polar media.<sup>5a</sup> As anticipated, the presence of vinyl and aryl substituents with electron

**Table 1. Computed B3LYP/6-31G(d,p) acidities for a series of catalysts without their counteranions.<sup>a</sup>**

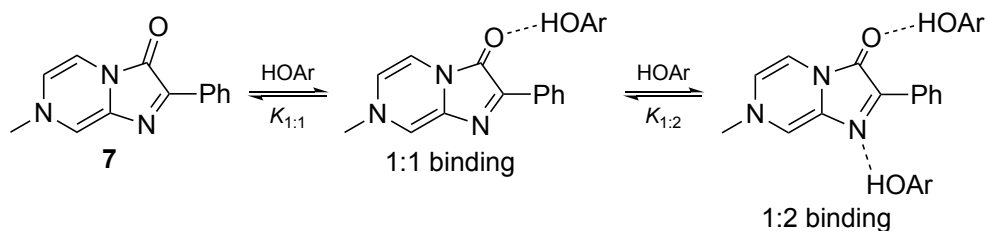
catalyst	$\Delta G^\circ_{\text{acid}}$	$\Delta\Delta G^\circ_{\text{acid}}$
<b>1</b>	232.9	0.0
<b>2</b>	230.9	-2.0
<b>4</b>	226.6	-6.3
<b>5</b>	224.2	-8.7
<b>6</b>	219.3	-13.6

<sup>a</sup>All values are given in kcal mol<sup>-1</sup> at 298 K. Smaller numbers for  $\Delta G^\circ_{\text{acid}}$  correspond to stronger acids.

withdrawing groups at the nitrogen ring center lead to more acidic species than their alkyl-substituted counterpart (i.e., **1**). In addition, **6**, the *para*-substituted analog of **4**, is the strongest acid in this series due to enhanced electron delocalization in its conjugate base.

Several spectroscopic approaches were carried out to experimentally evaluate the relative acidities and hydrogen bond donating abilities of **1–6**. Infrared spectroscopy was initially explored as previously reported by observing the change between the O–H stretching frequency of a phenol in carbon tetrachloride and upon coordination with 1% v/v CD<sub>3</sub>CN in CCl<sub>4</sub>.<sup>5a,5d</sup> A reduction in this mode from 3541 cm<sup>-1</sup> to 3128 cm<sup>-1</sup> was observed for **3**, and this difference of 413 cm<sup>-1</sup> is larger than the 370 cm<sup>-1</sup> reported for *N*-*n*-octyl-3-hydroxypyridinium BAr<sup>F</sup><sub>4</sub>.<sup>5a</sup> This result is consistent with an acidity enhancement due to the presence of an electron withdrawing group, but **2** and **4–6** are not soluble in carbon tetrachloride or in CD<sub>3</sub>CN/CCl<sub>4</sub> mixtures with up to 5% acetonitrile-*d*<sub>3</sub>. Consequently, we decided to focus on alternative approaches.

A UV-vis titration method for evaluating hydrogen bond donor ability utilizing 7-methyl-2-phenylimidazo[1,2-*a*]pyrazine-3(7H)-one (**7**) as a colorimetric sensor was first reported by Kozłowski and coworkers and recently updated by Payne and Kass.<sup>5d,10</sup> In the latter approach, a constant concentration of **7** is maintained as it is titrated with a Brønsted acid of interest (HOAr in this case). This leads to a blue-shift of the λ<sub>max</sub> of **7** due to its coordination with the hydrogen bond donor. When a 1:1 association occurs (Scheme 1), an isosbestic point is observed (Figures 2 and



**Scheme 1.** Coordination of **7** to afford 1:1 and 1:2 binding complexes.

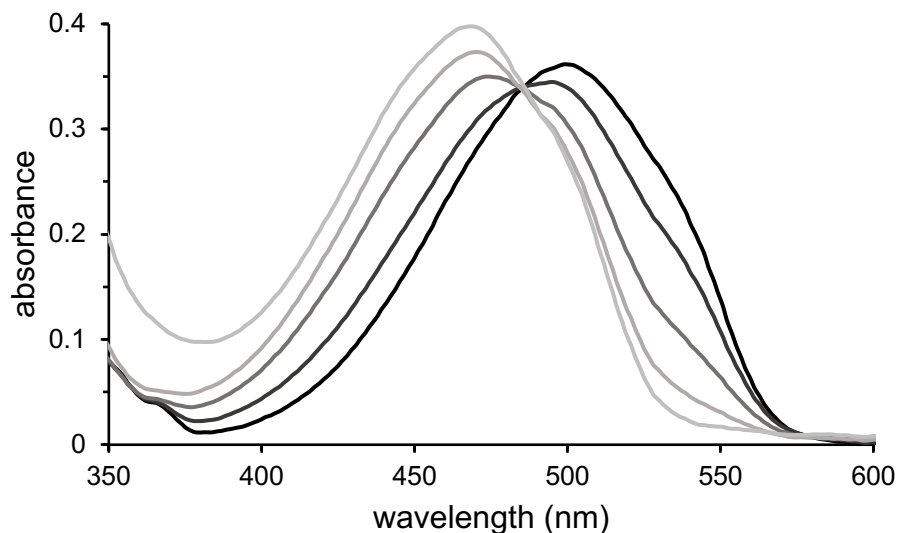


**Figure 2.** UV-vis spectra from 350 to 600 nm for the titration of **7** with **4**. Only some of the spectra are provided for clarity.

S8–S11) and a non-linear fit of the data affords the equilibrium binding constant ( $K_{1:1}$ , Table 2). This was the case for **1**, **2**, **4**, and **5**, but not **6**. An isosbestic point is not observed for this last compound (Figure 3) which is indicative of the formation of at least two intermediate species, and

**Table 2. Non-linear binding isotherm titration results for a series of catalysts with 7.<sup>a</sup>**

catalyst	$\lambda_{\max(1:1)}$ (nm) <sup>b</sup>	$K_{1:1}$	$K_{1:2}$
<b>1</b> <sup>c</sup>	472.1 (471.7)	$2.0 \times 10^4$	
<b>2</b>	469.4 (468.8)	$5.3 \times 10^4$	
<b>4</b>	469.1 (468.8)	$8.5 \times 10^4$	
<b>5</b>	466.3 (466.0)	$1.7 \times 10^5$	
<b>6</b>	434.7	$3.5 \times 10^5$	$7.2 \times 10^3$

<sup>a</sup>Constant sensor concentrations of 22–34  $\mu\text{M}$  in  $\text{CH}_2\text{Cl}_2$  were used. <sup>b</sup>Calculated values obtained from a plot of  $\chi/\lambda_{\max}$  at each titration point, where  $\chi$  is the 1:1 mole fraction resulting from the fit of the data. See ref. 5d for further details. Parenthetical numbers are the directly observed  $\lambda_{\max}$  values from the titrations. <sup>c</sup>Data from ref. 5d.

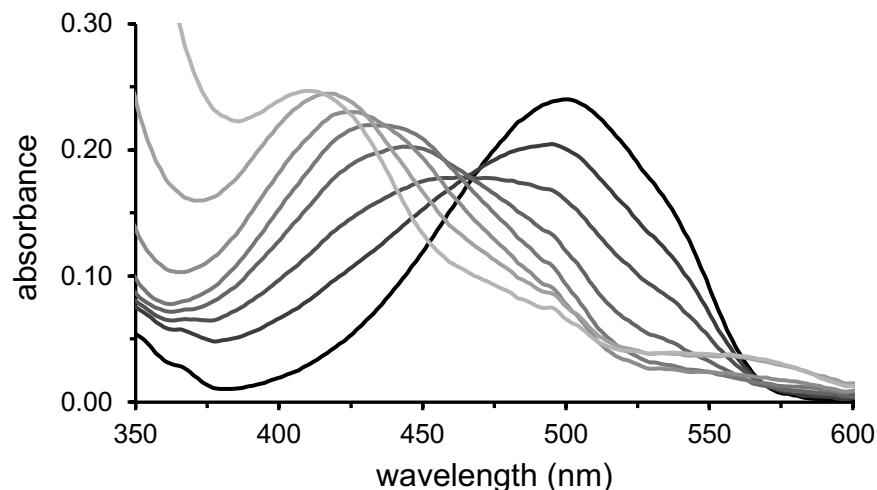


**Figure 3.** UV-vis spectra from 350 to 600 nm for the titration of **7** with **6**. Only some of the spectra are provided for clarity.

is consistent with the resulting 1:2 binding model fit of the titration results. A plot of the logarithm of  $K_{1:1}$  versus  $\Delta G^\circ_{\text{acid}}$  (Figure 4) is linear for all five hydroxypyridinium ion salts examined in this work, indicating that the 1:1 binding equilibrium constants provide a good measure of the catalysts' acidities and hydrogen bond donating abilities.<sup>11</sup>

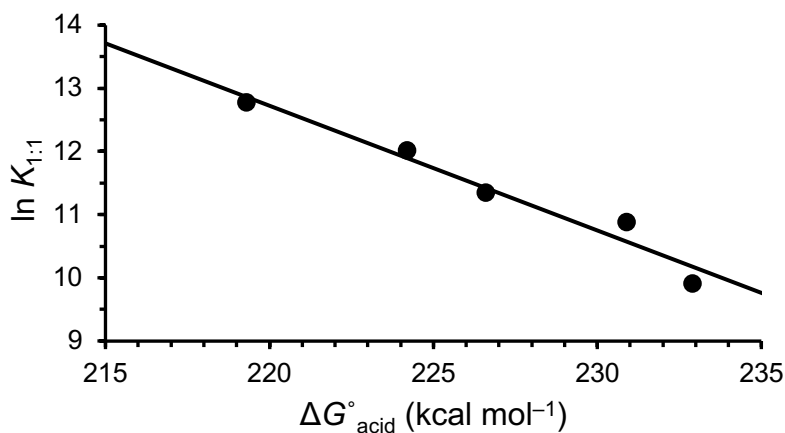


**Figure 4.** Logarithm of 1:1 equilibrium binding constants versus computed gas-phase acidities. A linear least-squares analysis affords  $\ln K_{1:1} = -0.198 \times \Delta G^\circ_{\text{acid}} + 56.2$ ,  $r^2 = 0.959$ .

An alternative spectroscopic approach for evaluating Brønsted acidities and hydrogen bond donating abilities in nonpolar media was reported by Diemoz and Franz this past year.<sup>12</sup> In this methodology, the <sup>31</sup>P NMR spectrum of triethylphosphine oxide (Et<sub>3</sub>PO) is recorded in dichloromethane and subsequently titrated with a Brønsted acid of interest. Rapid formation of a hydrogen bond complex leads to an averaged spectrum with a single downfield <sup>31</sup>P signal. Its chemical shift progressively increases until it levels off to a constant value as more of the acid is added and the proportion of free (non-complexed) Et<sub>3</sub>PO diminishes to negligible amounts. The magnitude of this shift ( $\Delta\delta$ ) was found to correlate with the activity of a variety of organocatalysts. For **1** it was found that only 1.5 equivalents are needed to bind to Et<sub>3</sub>PO to achieve the maximum downfield shift (Table S7). Since all of our other catalysts are predicted to be more acidic than **1**, 1.5 equivalents of these acids were considered to be sufficient to obtain the chemical shifts of the bound complexes (i.e.  $\delta_{1.5}$ ). A summary of the results is given in Table 3 and  $\Delta\delta$  for the *meta*-substituted isomers (**1**, **2**, **4**, and **5**) were found to linearly correlate with  $\ln K_{1:1}$  from the UV-vis data (Figure 5) and  $\Delta G^\circ_{\text{acid}}$  (i.e., the computed gas-phase acidities, Figure S14). The *para*-

**Table 3. Titration results for a series of catalysts with Et<sub>3</sub>PO monitored by <sup>31</sup>P NMR.<sup>a</sup>**

catalyst	$\delta_{1.5}$ (ppm) <sup>b</sup>	$\Delta\delta$ (ppm)
<b>1</b>	60.83	10.33
<b>2</b>	61.67	11.17
<b>4</b>	61.96	11.46
<b>5</b>	62.49	11.99
<b>6</b>	65.44	14.94

<sup>a</sup>Triethylphosphine oxide (5.0 mM) in CD<sub>2</sub>Cl<sub>2</sub> has a chemical shift of 50.50 ppm. <sup>b</sup>Observed chemical shifts upon addition of 1.5 equivalents of the indicated acid.

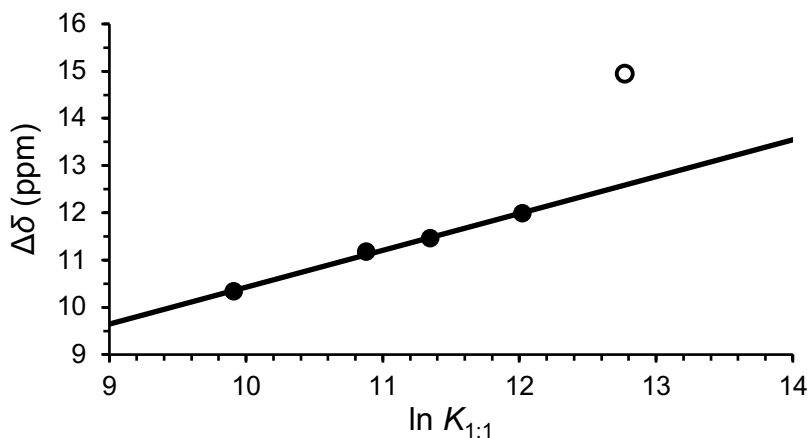


**Figure 5.** Triethylphosphine oxide  $^{31}\text{P}$  NMR shift changes versus  $\ln K_{1:1}$  for *meta*-substituted catalysts (filled circles) and **6** (open circle). A linear least-squares fit for the *meta* compounds gives the following equation:  $\Delta\delta$  (ppm) =  $0.781 \times \ln K_{1:1} + 2.62$ ,  $r^2 = 0.997$ .

substituted derivative shows positive deviations from the lines in both plots, presumably because of its enhanced acidity and hydrogen bond donating ability due to the conjugation of the acidic site with the formally charged nitrogen atom center.

Computations, 1:1 equilibrium binding constants from UV-vis titrations, and the triethylphosphine oxide  $^{31}\text{P}$  NMR data all predict a catalyst activity order of **6** > **5** > **4** > **2** > **1**. To assess this prognostication, the Friedel–Crafts alkylation of *N*-methylindole with *trans*- $\beta$ -nitrostyrene (eq. 1) was examined. This reaction was chosen because it is known to progress more rapidly with stronger acids in a related series and has been widely used to assess organocatalysts.<sup>5,12,13</sup> Pseudo-first order rate constants were obtained using  $^1\text{H}$  NMR to monitor the reaction progress (Table 4). The reaction rates increased as expected for the *meta*-substituted

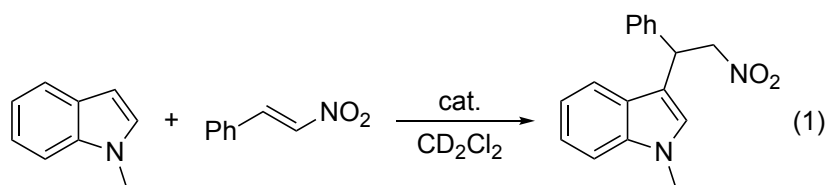
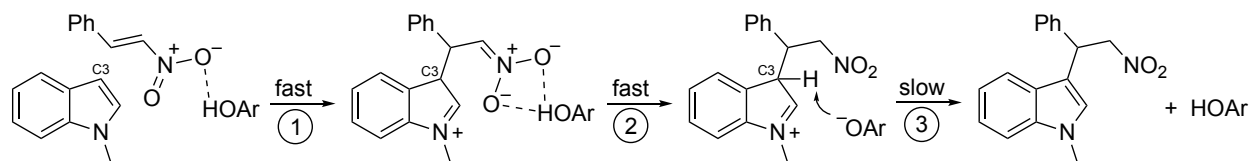


**Table 4. Kinetic data for the Friedel–Crafts alkylation of *N*-methylindole with *trans*- $\beta$ -nitrostyrene.<sup>a</sup>**

entry	catalyst	$k$ (h <sup>-1</sup> )	$t_{1/2}$ (h)	$k_{rel}$
1		$1.9 \times 10^{-4}$	3700	0.0023
2	<b>1</b>	0.082	8.5	1.0
3	<b>2</b>	0.17	4.2	2.0
4	<b>4</b>	0.19	3.6	2.4
5	<b>5</b>	0.29	2.4	3.6
6	<b>6</b>	0.21	3.3	2.6
7	TfOH	0.0088	79	0.11

<sup>a</sup>Reactions were carried out at 27 °C in CD<sub>2</sub>Cl<sub>2</sub> with 10 mol% of the indicated catalyst, 500 mM of *trans*- $\beta$ -nitrostyrene, and 50 mM of *N*-methylindole. Rate constants are corrected for the non-catalyzed background process.

pyridinium salts (i.e., **5** > **4** > **2** > **1**), but surprisingly, **6** afforded a smaller rate acceleration than **5** by a factor of 1.4, despite the former's greater acidity, larger  $K_{1:1}$ , and bigger  $\Delta\delta$ . Triflic acid was also examined, and it was found to be less active than our phenol derivatives and a poor catalyst for this transformation. This led us to hypothesize that for the stronger acids the carbon-carbon bond forming step in the Friedel–Crafts alkylation may no longer be rate determining, and that deprotonation at C3 to aromatize the indole and reform the catalyst could become the slow step (Scheme 2). Such variations with changing pH are well-known and have been reported with organocatalysts,<sup>14</sup> but not for the Friedel–Crafts reaction of *N*-methylindole with *trans*- $\beta$ -nitrostyrene even though it has been extensively used for benchmarking purposes.



**Scheme 2.** Proposed reaction mechanism for the Friedel–Crafts alkylation of *N*-methylindole with *trans*- $\beta$ -nitrostyrene where step 3 becomes rate determining with strong acid catalyts.

To probe a possible change in the rate determining step of the mechanism, isotopically labeled 3-deuterio-*N*-methylindole<sup>15</sup> was prepared and kinetic isotope effects (KIEs) for the Friedel–Crafts alkylation with different catalyts were determined (Table 5). An inverse KIE was obtained with **4**, and this is consistent with a rate determining carbon-carbon bond forming step (i.e., a change in hybridization from  $sp^2$  to  $sp^3$  in the nucleophilic attack of *N*-methylindole on *trans*- $\beta$ -nitrostyrene). Conversely, normal KIEs were found with **6** and triflic acid. This is in accord with the deprotonation at C3 becoming the slow step in the reaction mechanism when more acidic catalyts are used. No isotope effect was found with **5**, suggesting that nucleophilic attack and

**Table 5. Kinetic data for the Friedel–Crafts alkylation of 3-deuterio-*N*-methylindole with *trans*- $\beta$ -nitrostyrene.<sup>a</sup>**

entry	catalyst	$k_D$ ( $h^{-1}$ )	$t_{1/2}$ (h)	K.I.E.
1	<b>4</b>	0.24	2.8	0.80
2	<b>5</b>	0.29	2.4	1.0
3	<b>6</b>	0.13	5.2	1.6
4	TfOH	0.0050	138	1.7

<sup>a</sup>Background corrected initial rates corresponding to reaction conversions of  $\leq 10\%$  were obtained at 27 °C in  $CDCl_2$  using 50 mM of 3-deuterio-*N*-methylindole, 500 mM *trans*- $\beta$ -nitrostyrene, and 10 mol% of the indicated catalyts.

deprotonation are competitive in this case. In accord with the proposed mechanism in Scheme 2,  $^2\text{H}$  NMR experiments showed that deuterium was only incorporated into the product at the  $\alpha$ -position to the nitro group and was not observed until greater than 10% conversion to the product was reached. These findings reveal that the reaction rate for the Friedel–Crafts alkylation is not a reliable indicator of relative acidities for acidic catalysts.

It was anticipated that a more acidic intermediate in the Friedel–Crafts reaction is formed when 2,2,2-trifluoroacetophenone is used as the electrophile in lieu of *trans*- $\beta$ -nitrostyrene. Two electron withdrawing groups are present in the former case rather than one (i.e., OH and  $\text{CF}_3$  vs  $\text{NO}_2$ ) and they both are one bond closer to the key C3 position. This should facilitate the re-aromatization step (3 in Scheme 2) making it more likely that carbon-carbon bond formation will be rate determining, and increasing the acidity range of catalysts that can be reliably probed. Mono- and bis-coupled products are commonly observed for this transformation (eq. 2)<sup>16</sup> and so the selectivities along with the reaction rate constants are given in Table 6 for the least (**1**) and most (**5**, **6**, and TfOH) acidic catalysts that were explored in this study. As expected, the KIEs are smaller for each catalyst, and this transformation proceeds 3.5 times more rapidly with **6** than with **5**. Formation of the bis-coupled product increases with the catalytic activity suggesting that the mono : bis ratio can also serve as an indicator of the catalysts' relative acidities. Tunable catalysts with modular syntheses such as our hydroxypyridinium salts are useful for this type of reaction since the proper balance between reaction rate and selectivity must be struck.

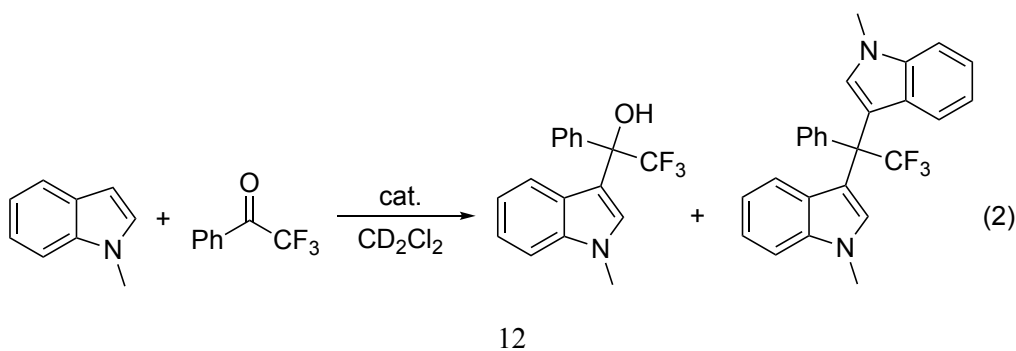


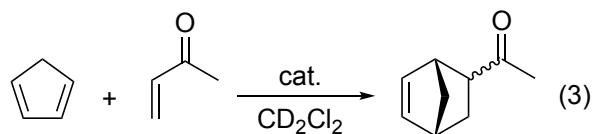
**Table 6. Kinetic and selectivity data for the Friedel–Crafts reaction of *N*-methylindole with 2,2,2-trifluoroacetophenone.<sup>a</sup>**

entry	cat.	$k_H$ (h <sup>-1</sup> )	$t_{1/2}$ (h)	$k_{rel}$	mono:bis <sup>b</sup>	$k_D$ (h <sup>-1</sup> ) <sup>c</sup>	$t_{1/2}$ (h)	$k_H/k_D$
1		$7.4 \times 10^{-5}$	9400	0.0010	100:0			
2	<b>1</b>	0.072	10	1	100:0			
3	<b>5</b>	0.34	2.1	4.6	98:2	0.38	1.8	0.90
4	<b>6</b>	1.1	0.61	16	91:9	0.95	0.73	1.2
5	TfOH	0.053	13	0.73	86:14	0.037	19	1.4

<sup>a</sup>Reactions were carried out at 27 °C in CD<sub>2</sub>Cl<sub>2</sub> with 500 mM of 2,2,2-trifluoroacetophenone, 50 mM of *N*-methylindole or 3-deuterio-*N*-methylindole, and 10 mol% of the indicated catalyst.

<sup>b</sup>The product selectivities were determined using *N*-methylindole. <sup>c</sup>Initial rates were used.

To avoid multistep mechanisms where the rate determining step can change with the acidity of the catalyst, and to examine a model transformation that better reflects the Brønsted acidity and hydrogen bond donating ability of the catalyst, the Diels–Alder reaction between cyclopentadiene and methyl vinyl ketone was examined (eq. 3). Pseudo-first order rate constants and the *endo:exo*



product ratios were measured at 25 °C in dichloromethane-*d*<sub>2</sub> with a 1 mol% catalyst loading (Table 7). As expected based upon the computed acidities, UV-vis and <sup>31</sup>P NMR data, the reactivity order is now **6** > **5** > **4** > **1** and the selectivities follow a similar trend. Excellent correlations between ln  $k$  and  $\Delta\delta$ , ln  $K_{1:1}$ , and  $\Delta G^\circ_{acid}$  are observed (Figures 6, S15 and S16), indicating that all three approaches can serve as useful guides for catalytic activities.

**Table 7. Kinetic and selectivity data for the Diels–Alder reaction of cyclopentadiene with methyl vinyl ketone.<sup>a</sup>**

entry	catalyst	$k$ (h <sup>-1</sup> )	$t_{1/2}$ (h)	$k_{rel}$	<i>endo:exo</i>
1		0.11	6.5	0.72	86:14
2	<b>1</b>	0.15	4.7	1	89:11
3	<b>4</b>	0.46	1.5	3.1	91:9
4	<b>5</b>	0.81	0.85	5.5	91:9
5	<b>6</b>	3.4	0.20	23	92:8

<sup>a</sup>Reactions were carried out at 25 °C in CD<sub>2</sub>Cl<sub>2</sub> with 1 mol% of the indicated catalyst, 250 mM cyclopentadiene, and 25 mM methyl vinyl ketone. Background corrected rate constants for the non-catalyzed process are given.

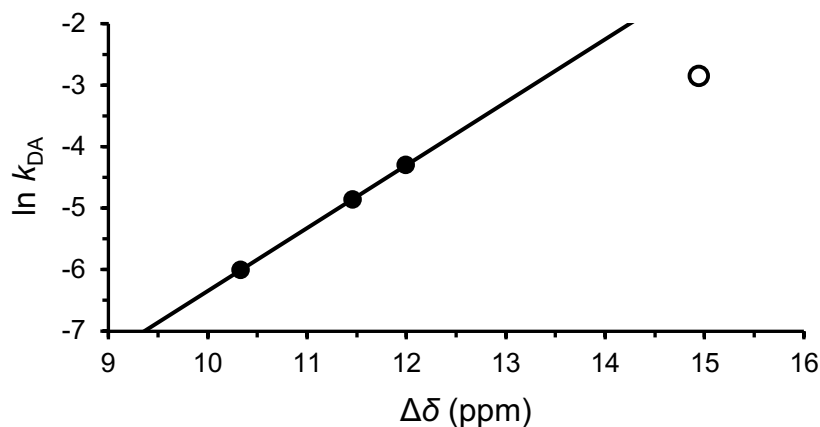


**Figure 6.** A plot of the logarithm of the rate constant for the Diels–Alder reaction of cyclopentadiene with methyl vinyl ketone vs  $\Delta\delta$  of the Et<sub>3</sub>PO<sup>31</sup>P NMR shift for *meta*-substituted catalysts (filled circles) and the *para*-isomer **6** (open circle). Linear least squares fits of the data give  $\ln k = 1.02 \times \Delta\delta - 16.6$ ,  $r^2 = 1.00$  (*meta* isomers only) and  $\ln k = 0.650 \times \Delta\delta - 12.4$ ,  $r^2 = 0.955$  (all compounds).

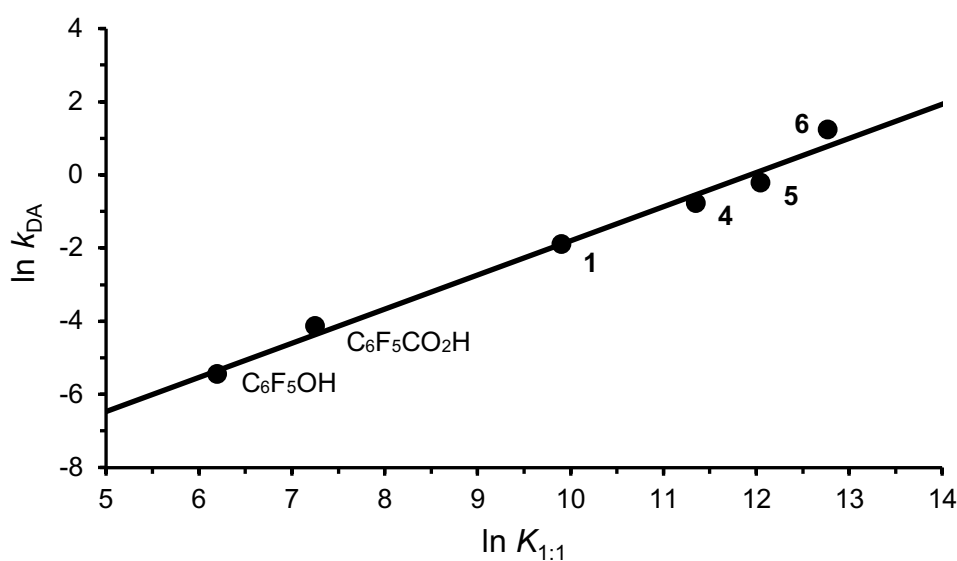
A comparison of the charge-activated catalysts with non-charged species would be useful to obtain a better sense of their qualitative acidities. Pentafluorophenol (C<sub>6</sub>F<sub>5</sub>OH) and pentafluorobenzoic acid (C<sub>6</sub>F<sub>5</sub>CO<sub>2</sub>H) were chosen for this purpose because they have known equilibrium association constants with  $7^{10}$  and  $\Delta\delta$  <sup>31</sup>P NMR shifts with Et<sub>3</sub>PO,<sup>12</sup> and the latter values for pentafluorophenol and pentafluorobenzoic acid are between those for **1** and **4**, and **5** and **6**, respectively (Table 8). The UV-vis method, however, suggests that the two non-charged compounds are significantly weaker acids than the hydroxypyridinium salts, and should be much less effective catalysts. Kinetic data for both the Friedel–Crafts alkylation of *N*-methylindole with *trans*- $\beta$ -nitrostyrene and the Diels–Alder reaction of cyclopentadiene with methyl vinyl ketone were obtained using both C<sub>6</sub>F<sub>5</sub>OH and C<sub>6</sub>F<sub>5</sub>CO<sub>2</sub>H. The resulting rate constants for the latter reaction are in accord with the *K*<sub>1:1</sub> values from the UV-vis titrations in that the two non-charged

**Table 8. Spectroscopic and kinetic data for the Friedel–Crafts and Diels–Alder reactions with all catalysts.**

catalyst	<i>K</i> <sub>1:1</sub>	$\Delta\delta$ (ppm)	<i>k</i> <sub>FC</sub> (h <sup>-1</sup> ) <sup>a</sup>	<i>t</i> <sub>1/2</sub> (h)	<i>k</i> <sub>DA</sub> (h <sup>-1</sup> ) <sup>b</sup>	<i>t</i> <sub>1/2</sub> (h)
<b>1</b>	$2.0 \times 10^4$	10.33	0.082	8.5	0.15	4.7
<b>4</b>	$8.5 \times 10^4$	11.46	0.19	3.6	0.46	1.5
<b>5</b>	$1.7 \times 10^5$	11.99	0.29	2.4	0.81	0.85
<b>6</b>	$3.5 \times 10^5$	14.94	0.21	3.3	3.4	0.20
C <sub>6</sub> F <sub>5</sub> OH	492 <sup>c</sup>	11.0 <sup>d</sup>	0.00043	1600	0.0043	160
C <sub>6</sub> F <sub>5</sub> CO <sub>2</sub> H	1410 <sup>c</sup>	12.8 <sup>d</sup>	0.0042	160	0.016	43

<sup>a</sup>Reactions were carried out at 27 °C in CD<sub>2</sub>Cl<sub>2</sub> with 10 mol% of the indicated catalyst, 500 mM *trans*- $\beta$ -nitrostyrene, and 50 mM *N*-methylindole. <sup>b</sup>Reactions were carried out at 25 °C in CD<sub>2</sub>Cl<sub>2</sub> with 1 mol% of the indicated catalyst, 250 mM cyclopentadiene, and 25 mM methyl vinyl ketone. Background corrected rate constants for the non-catalyzed processes are given. <sup>c</sup>This value comes from ref. 10. <sup>d</sup>This value was taken from ref. 12.

1  
2  
3 catalysts are much less effective than **1**, **4**, **5**, and **6**.<sup>17</sup> Both of these quantities ( $k$  and  $K_{1:1}$ ) span  
4  
5 approximately three orders of magnitude and their log-log plot is linear for all six catalysts that  
6  
7 were examined (i.e., charged and non-charged, Figure 7). An analogous correlation with the <sup>31</sup>P  
8  
9 NMR  $\Delta\delta$  shifts is not observed indicating that binding to Et<sub>3</sub>PO is not as universal a predictor of  
10  
11 reactivity, and depends more on the structure of the species being investigated (i.e., compounds  
12  
13 with the same  $\Delta\delta$  values can have different acidities and catalytic activities). This is in keeping  
14  
15 with the report by Diemoz and Franz, who found separate correlations for different types of  
16  
17 compounds.<sup>12</sup>  
18  
19  
20  
21  
22  
23  
24  
25



26  
27  
28  
29  
30  
31  
32  
33  
34  
35  
36  
37  
38  
39  
40  
41  
42  
43  
44  
45  
46 **Figure 7.** A plot of the logarithm of the rate constant for the Diels–Alder reaction of  
47 cyclopentadiene with methyl vinyl ketone vs the logarithm of the 1:1 equilibrium binding constants  
48 with colorimetric sensor **7** for all six catalysts in Table 8. The equation for the line obtained from  
49 a linear least squares fit is  $\ln k_{DA} = 0.934 \times \ln K_{1:1} - 11.1$ ,  $r^2 = 0.987$ .  
50  
51  
52  
53  
54  
55  
56  
57  
58  
59  
60

1  
2  
3  
4  
5  
6  
7  
8  
9  
10  
11  
12  
13  
14  
15  
16  
17  
18  
19  
20  
21  
22  
23  
24  
25  
26  
27  
28  
29  
30  
31  
32  
33  
34  
35  
36  
37  
38  
39  
40  
41  
42  
43  
44  
45  
46  
47  
48  
49  
50  
51  
52  
53  
54  
55  
56  
57  
58  
59  
60

If one uses the Friedel–Crafts rate constants for the transformation of *N*-methylindole with *trans*- $\beta$ -nitrostyrene rather than those for the Diels–Alder reaction of cyclopentadiene with methyl vinyl ketone in the log-log plot displayed in Figure 7, then a parabolic relationship results rather than a straight line (Figure 8). The maximum rate is obtained with **5** and falls off with more or less acidic catalysts as given by bigger or smaller  $K_{1:1}$  values, respectively. This indicates that **5** represents an inflection point in the mechanism and the rate determining step shifts from C–C bond formation with weaker acids to proton abstraction with stronger ones (i.e., steps 1 vs 3 in Scheme 2). In accord with this view, the kinetic isotope effects are 1.0 for **5**,  $< 1.0$  for weaker acids and  $> 1.0$  for stronger ones. It also appears that the charged hydroxypyridinium ion salts are all more acidic than trifluoroacetic acid ( $\text{CF}_3\text{CO}_2\text{H}$ ) given that  $K_{1:1} = 5,490$  and  $\ln K_{1:1} = 8.61$  for this compound.<sup>10,18</sup>

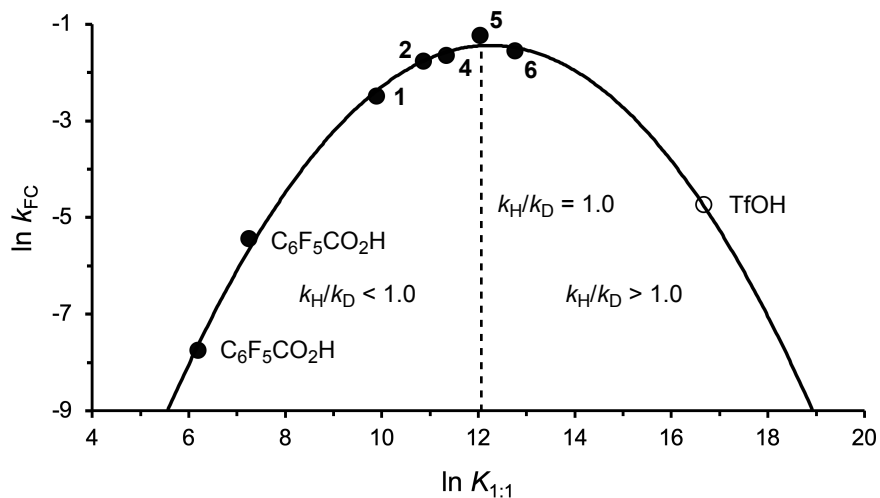


**Figure 8.** A plot of the logarithm of the rate constant for the Friedel–Crafts reaction of *N*-methylindole with *trans*- $\beta$ -nitrostyrene versus the logarithm of the 1:1 equilibrium binding constants with colorimetric sensor **7** (filled circles). A least squares analysis of the data gives  $\ln k_{DA} = -0.169 \times (\ln K_{1:1})^2 + 4.15 \times \ln K_{1:1} - 26.8$ ,  $r^2 = 0.996$ , and this quadratic equation was used to obtain an estimated value for  $\ln K_{1:1}$  for triflic acid (open circle) of 16.6.

## CONCLUSION

Incorporation of electron withdrawing substituents into charge-containing catalysts proved to be an effective strategy for increasing their acidities in a nonpolar solvent ( $\text{CH}_2\text{Cl}_2$ ) as measured by 1:1 equilibrium association constants with **7**,  $^{31}\text{P}$  NMR shifts with triethylphosphine oxide, and gas-phase acidities. Of these quantities, the  $K_{1:1}$  values were found to be more broadly suitable for correlating catalyst activities. Kinetic isotope effects and an inverted parabolic rate profile for the Friedel–Crafts alkylation of *N*-methylindole with *trans*- $\beta$ -nitrostyrene revealed that the rate determining step can change from carbon-carbon bond formation to proton transfer to the conjugate base of the catalyst. This leads to a region where reaction rates decrease with increasing acidity making this a less useful model transformation for evaluating relative catalyst acidities than previously considered. All of the hydroxypyridinium  $\text{BAr}^{\text{F}_4^-}$  salts reported in this work were also found to be more acidic in dichloromethane than trifluoroacetic acid.

## EXPERIMENTAL

**General.** All reaction vessels and NMR tubes were stored at 120 °C for a minimum of 12 h and allowed to cool to room temperature in a vacuum desiccator over Drierite before use. Syringes and volumetric flasks were kept in the same desiccator but were not heated. Alumina, molecular sieves, and calcium sulfate were activated in a kiln at 300 °C for at least 24 h.

Acetone, chloroform, and carbon tetrachloride were supplied by Fisher Scientific whereas ethyl propiolate, 2,2,2-trifluoroacetophenone, and pentafluorobenzoic acid were obtained from Oakwood Chemical. 1-Chloro-2,4-dinitrobenzene, triethylphosphine oxide, sodium tetrakis[3,5-bis(trifluoro-methyl)phenyl]borate ( $\text{NaBAr}^{\text{F}_4}$ ), pentafluorophenol, and HCl were purchased from

1  
2  
3 Across Organics, Alfa Aesar, ArkPharm, Fluka, and VWR Chemical, respectively. Deuterated  
4 solvents were acquired from Cambridge Isotope Laboratories and all other chemicals came from  
5 Sigma-Aldrich. Reagents were used as supplied except for *N*-methylindole, which was passed neat  
6 through a pipet containing activated alumina and stored under argon. Anhydrous CH<sub>2</sub>Cl<sub>2</sub> was used  
7 as purchased, CD<sub>2</sub>Cl<sub>2</sub> was dried by the addition of activated molecular sieves to the reagent bottle  
8 at least 24 h before use, and all other solvents were dried in the same manner as *N*-methylindole  
9 and stored over molecular sieves. Charged catalysts were kept under vacuum (0.05–0.1 Torr) for  
10 at least 12 h before use.

11  
12 NMR spectra were obtained with 400 and 500 MHz spectrometers. The <sup>1</sup>H and <sup>13</sup>C chemical  
13 shifts were referenced at  $\delta$  5.32 and 54.0 (CD<sub>2</sub>Cl<sub>2</sub>),  $\delta$  7.26 and 77.2 (CDCl<sub>3</sub>),  $\delta$  2.50 and 39.5  
14 (DMSO-*d*<sub>6</sub>), and  $\delta$  1.94 and 1.3 (CD<sub>3</sub>CN), respectively. <sup>2</sup>H chemical shifts were referenced relative  
15 to benzene-*d*<sub>6</sub> (7.36 ppm). Triethylphosphine oxide <sup>31</sup>P NMR shifts were acquired in CD<sub>2</sub>Cl<sub>2</sub> and  
16 referenced at  $\delta$  50.5 through the deuterium lock channel according to the IUPAC unified scale.<sup>19</sup>  
17  
18 Medium pressure liquid chromatography was performed using an automated flash chromatography  
19 system with silica gel columns. Melting point data were collected in unsealed capillaries and were  
20 uncorrected. Solution and ATR FT-IR spectra were recorded with a liquid cell and a laminated  
21 diamond crystal, respectively. High resolution mass spectra were obtained with an electrospray  
22 ionization - time of flight mass spectrometer using PEG-200 as an internal mass calibrant. UV  
23 spectra were taken using 10 mm quartz cells sealed with PTFE septum caps.

24  
25 ***N*-Methyl-3-hydroxypyridinium (1).** The iodide and BAr<sup>F</sup><sub>4</sub><sup>-</sup> salts of this ion were prepared  
26 according to the literature procedure.<sup>5d</sup>

27  
28 **(*E*)-*N*-(2-Carboethoxyvinyl)-3-hydroxypyridinium BAr<sup>F</sup><sub>4</sub> (2).** Concentrated HCl (1.75 mL,  
29 21.0 mmol) was added dropwise with stirring to a 50 mL round-bottomed flask containing 3-

hydroxypyridine (1.00 g, 10.5 mmol) and 25 mL of methanol. After 10 min, the solvent was removed in vacuo and the resulting solid was dissolved in ethanol (30 mL). Ethyl propiolate (1.60 mL, 1.55 g, 15.8 mmol) was added and this mixture was heated with an oil bath to reflux overnight. Concentration of the resulting material with a rotary evaporator afforded a residue which was dissolved in 25 mL of acetone. This solution was stirred overnight at room temperature and the resulting precipitate was isolated by vacuum filtration to give 845 mg (35%) of crude **2-Cl**. Some of this material (64.7 mg, 0.282 mmol), along with 1.5 mL of CH<sub>2</sub>Cl<sub>2</sub> and 250 mg (0.28 mmol) of NaBAr<sup>F</sup><sub>4</sub>, were added to a 6 dram vial and stirred overnight at room temperature. The resulting precipitate was removed with a 0.45 μm PTFE membrane and then hexanes were added until the solution just became cloudy. This mixture was subsequently dried over activated CaSO<sub>4</sub> and filtered through another 0.45 μm PTFE membrane. Removal of the solvent in vacuo gave 253 mg (85%) of an off-white powder (mp 175–178 °C) which was stored in a dry-box under nitrogen. <sup>1</sup>H NMR (400 MHz, CD<sub>2</sub>Cl<sub>2</sub>) δ 8.35 (dd, *J* = 2.2, 1.7 Hz, 1H), 8.28 (ddd, *J* = 6.0, 1.2, 1.2 Hz, 1H), 8.10 (ddd, *J* = 8.8, 2.5, 1.0 Hz, 1H), 8.05 (d, *J* = 13.9 Hz, 1H), 7.99 (dd, *J* = 8.8, 6.0 Hz, 1H), 7.72 (s, 8H), 7.56 (s, 4H), 6.74 (d, *J* = 14.0 Hz, 1H), 4.37 (q, *J* = 7.1 Hz, 2H), 1.36 (t, *J* = 7.1 Hz, 3H). <sup>13</sup>C {<sup>1</sup>H} NMR (125 MHz, CD<sub>2</sub>Cl<sub>2</sub>) δ 162.5, 162.3 (q, <sup>1</sup>J<sub>B-C</sub> = 62 Hz), 158.4, 141.5, 136.0, 135.4, 133.8, 130.2, 130.1, 129.4 (qq, <sup>2</sup>J<sub>F-C</sub> = 39 Hz and <sup>2</sup>J<sub>B-C</sub> = 3.5 Hz), 125.2 (q, <sup>1</sup>J<sub>F-C</sub> = 339 Hz), 123.8, 118.1 (septet, <sup>3</sup>J<sub>F-C</sub> = 4.6 Hz), 63.6, 14.3. IR-ATR 3103, 1704, 1358, 1280, 1121 cm<sup>-1</sup>. HRMS (ESI) *m/z* [M – BAr<sup>F</sup><sub>4</sub>]<sup>+</sup> calcd for C<sub>10</sub>H<sub>12</sub>NO<sub>3</sub> 194.0812, found 194.0829.

***n*-Octyl (*E*)-3-chloroacrylate.** Propiolic acid (3.0 mL, 3.41 g, 48 mmol) was added over 1 min to a 25 mL round-bottomed flask containing 5 mL (60 mmol) of concentrated HCl. This solution was then heated with an oil bath to reflux with stirring for 18 h before being diluted with 5 mL of water. The product was extracted with chloroform (3 × 5 mL) and the combined organic material was

1  
2  
3 washed with brine ( $2 \times 5$  mL) and dried over  $\text{MgSO}_4$ . Concentration in vacuo gave 4.72 g (90%)  
4  
5 of crude (*E*)-3-chloroacrylic acid as an odorous, lustrous brown solid (flakes). A portion of this  
6  
7 material (450 mg, 4.1 mmol), along with 700  $\mu\text{L}$  (580 mg, 4.5 mmol) of *n*-octanol, and 160 mg  
8  
9 (0.84 mmol) of *p*-toluenesulfonic acid monohydrate, were placed in a 25 mL round-bottomed flask  
10  
11 equipped with a Dean-Stark trap and dissolved in 7.5 mL of toluene. This solution was heated with  
12  
13 an oil bath to 130  $^\circ\text{C}$  for 24 h, during which time water was removed from the system.  
14  
15 Concentration of the reaction mixture with a rotary evaporator was followed by addition of 15 mL  
16  
17 of hexanes and filtration of the resulting material. Removal of the solvent in vacuo afforded an oil  
18  
19 that was purified by MPLC with 5% ethyl acetate in hexanes to give 829 mg (92%) of a clear, pale  
20  
21 yellow liquid. The  $^1\text{H}$  NMR spectrum of this previously reported compound matched the literature  
22  
23 data.<sup>20</sup>  $^1\text{H}$  NMR (400 MHz,  $\text{CDCl}_3$ )  $\delta$  7.35 (d,  $J = 13.5$  Hz, 1H), 6.24 (d,  $J = 13.5$  Hz, 1H), 4.15 (t,  
24  
25  $J = 6.7$  Hz, 2H), 1.65 (p,  $J = 7.6$  Hz, 2H), 1.39–1.22 (m, 10H), 0.88 (t,  $J = 6.7$  Hz, 3H).  
26  
27  
28  
29

30  
31 **(*E*)-*N*-(2-Carbooctoxyvinyl)-3-hydroxypyridinium chloride (3-Cl).** In a 25 mL round-  
32  
33 bottomed flask, 779 mg (3.56 mmol) of *n*-octyl (*E*)-3-chloroacrylate and 271 mg (2.85 mmol) of  
34  
35 3-hydroxypyridine were dissolved in 5 mL of acetonitrile. This solution was heated to reflux with  
36  
37 an oil bath with stirring for 24 h, and then an additional 162 mg (0.741 mmol) of *n*-octyl (*E*)-3-  
38  
39 chloroacrylate was added. The reaction was heated for another 12 h and was subsequently  
40  
41 concentrated with a rotary evaporator. Ethyl acetate (10 mL) was added to the resulting dark brown  
42  
43 oil and the mixture was stirred at room temperature for 4 h. This resulted in precipitation of the  
44  
45 product, which was collected by vacuum filtration to afford 385 mg (43%) of a pale tan powder  
46  
47 (mp 132–134  $^\circ\text{C}$ ) that was stored in a dry-box under nitrogen.  $^1\text{H}$  NMR (400 MHz,  $\text{CDCl}_3$ )  
48  
49  $\delta$  9.31 (s, 1H), 8.59 (s, 1H), 8.33–8.20 (m, 2H), 7.95 (s, 1H), 6.95 (d,  $J = 13.4$  Hz, 1H),  
50  
51 4.23 (t,  $J = 6.7$  Hz, 2H), 1.70 (p,  $J = 6.8$  Hz, 2H), 1.41–1.20 (m, 10H), 0.87 (t,  $J = 6.8$  Hz, 3H).  
52  
53  
54  
55  
56  
57  
58  
59  
60

<sup>13</sup>C{<sup>1</sup>H} NMR (156 MHz, CDCl<sub>3</sub>) δ 163.3, 159.4, 142.3, 136.1, 132.8, 130.2, 128.9, 121.5, 66.7, 31.9, 29.30, 29.28, 28.6, 25.9, 22.8, 14.2. IR-ATR 2958, 2928, 2855, 2473 (OH···Cl), 1710, 1582, 1317, 1289, 1185 cm<sup>-1</sup>. HRMS (ESI) *m/z* [M – Cl]<sup>+</sup> calcd for C<sub>16</sub>H<sub>24</sub>NO<sub>3</sub> 278.1751, found 278.1768.

**(E)-N-(2-Carbooctoxyvinyl)-3-hydroxypyridinium BAR<sup>F</sup><sub>4</sub> (3).** Dichloromethane (1 mL) was added to a 6 dram vial containing 565 mg (0.638 mmol) of NaBAR<sup>F</sup><sub>4</sub> and 200 mg (0.637 mmol) of **3-Cl** and the solution was stirred at room temperature overnight. Filtration of the resulting mixture through a 0.45 μm PTFE membrane and removal of the solvent under reduced pressure gave 720 mg (99%) of the product as an orange-brown semisolid. This material degraded with a half-life of approximately 5 days when stored in a dry-box under nitrogen. <sup>1</sup>H NMR (400 MHz, CD<sub>2</sub>Cl<sub>2</sub>) δ 8.34 (t, *J* = 2.0 Hz, 1H), 8.21 (dt, *J* = 6.0 and 2.0 Hz, 1H), 8.08 (ddd, *J* = 8.8, 2.5, and 1.0 Hz, 1H), 8.03 (d, *J* = 14.0 Hz, 1H), 7.89 (dd, *J* = 8.8 and 6.0 Hz, 1H), 7.75–7.70 (m, 8H), 7.57 (s, 4H), 6.73 (d, *J* = 14.0 Hz, 1H), 4.30 (t, *J* = 6.8 Hz, 2H), 1.73 (p, *J* = 7.4 Hz, 2H), 1.45–1.25 (m, 10H), 0.88 (t, *J* = 7.0 Hz, 3H). <sup>13</sup>C{<sup>1</sup>H} NMR (125 MHz, CDCl<sub>3</sub>) 162.1, 161.8 (q, <sup>1</sup>*J*<sub>B-C</sub> = 62 Hz), 158.1, 140.9, 135.1, 134.9, 132.5, 129.4, 129.2 (qq, <sup>2</sup>*J*<sub>F-C</sub> = 39 Hz and <sup>2</sup>*J*<sub>B-C</sub> = 3.8 Hz), 129.3, 124.6 (q, <sup>1</sup>*J*<sub>F-C</sub> = 338 Hz), 123.3, 117.7, 67.6, 31.8, 29.21, 29.17, 28.4, 25.8, 22.7, 14.1. IR-ATR 3084, 2933, 2861, 1706, 1582, 1355, 1277, 1127 cm<sup>-1</sup>. HRMS (ESI) *m/z* [M – BAR<sup>F</sup><sub>4</sub>]<sup>+</sup> calcd for C<sub>16</sub>H<sub>24</sub>NO<sub>3</sub> 278.1751, found 278.1759.

**N-(2,4-Dinitrophenyl)-3-hydroxypyridinium BAR<sup>F</sup><sub>4</sub> (4).** In a 50 mL round-bottomed flask, 320 mg (3.4 mmol) of 3-hydroxypyridine and 690 mg (3.4 mmol) of 1-chloro-2,4-dinitrobenzene were dissolved in 20 mL of acetonitrile and heated to reflux with an oil bath with stirring overnight. After cooling to room temperature, the resulting precipitate was collected by vacuum filtration and washed with acetonitrile to give 959 mg (96%) of crude **4-Cl** as a light tan powder. A portion of

1  
2  
3 this material (112 mg, 0.377 mmol) was dissolved in 5 mL of water with 300 mg (0.34 mmol) of  
4 NaBAR<sup>F</sup><sub>4</sub> in a 6 dram vial. Dichloromethane (5 mL) was added and the mixture was stirred  
5  
6 vigorously for 3 h. The clear yellow organic layer was subsequently washed with brine (2 × 5 mL)  
7  
8 and dried over MgSO<sub>4</sub>. It was then triturated with hexanes until the solution just became cloudy  
9  
10 whereupon it was passed through a 0.45 μm PTFE membrane. Removal of the solvent in vacuo  
11  
12 gave 328 mg (86%) of a light tan powder (mp 54–56 °C) which was stored in a dry-box under  
13  
14 nitrogen. <sup>1</sup>H NMR (400 MHz, CD<sub>2</sub>Cl<sub>2</sub>) δ 9.30 (d, *J* = 2.4 Hz, 1H), 8.85 (dd, *J* = 8.6 and 2.4 Hz,  
15  
16 1H), 8.25–8.19 (m, 2H), 8.14 (ddd, *J* = 6.0, 1.4, and 1.3 Hz, 1H), 8.07 (dd, *J* = 8.6 and 5.9 Hz,  
17  
18 1H), 7.93 (d, *J* = 8.6 Hz, 1H), 7.72 (s, 8H), 7.55 (s, 4H). <sup>13</sup>C{<sup>1</sup>H} NMR (125 MHz, CD<sub>2</sub>Cl<sub>2</sub>) δ  
19  
20 162.3 (q, <sup>1</sup>*J*<sub>B-C</sub> = 62 Hz), 159.7, 150.7, 143.7, 138.6, 136.7, 135.6, 135.4, 133.4, 131.1, 130.7,  
21  
22 130.0, 129.4 (qq, <sup>2</sup>*J*<sub>F-C</sub> = 39 Hz and <sup>2</sup>*J*<sub>B-C</sub> = 3.7 Hz), 125.2 (q, <sup>1</sup>*J*<sub>F-C</sub> = 339 Hz), 123.6, 118.1 (septet,  
23  
24 <sup>3</sup>*J*<sub>F-C</sub> = 5.0 Hz). IR-ATR 3114, 1694, 1611, 1553, 1481, 1354, 1279 cm<sup>-1</sup>. HRMS (ESI) *m/z* [M –  
25  
26 BAR<sup>F</sup><sub>4</sub>]<sup>+</sup> calcd for C<sub>11</sub>H<sub>8</sub>N<sub>3</sub>O<sub>5</sub> 262.0458, found 262.0467.

27  
28  
29  
30  
31  
32  
33 **(*E*)-*N*-(2-Cyanovinyl)-3-hydroxypyridinium BAR<sup>F</sup><sub>4</sub> (5).** A solution of 5.0 mL (4.1 g, 76 mmol)  
34  
35 of acrylonitrile in 5 mL of chloroform was prepared in a 25 mL round-bottomed flask fitted with  
36  
37 a condenser topped with an addition funnel. This setup was covered in aluminum foil to avoid  
38  
39 exposure to light and heated to reflux with an oil bath. Bromine (9.0 mL, 28g, 153 mmol) was then  
40  
41 added dropwise over 1 h and the reaction mixture was refluxed for an additional 3 h. It was  
42  
43 subsequently washed with 10% aqueous Na<sub>2</sub>S<sub>2</sub>O<sub>3</sub> (3 × 5 mL) and brine (2 × 5 mL), and then dried  
44  
45 with Na<sub>2</sub>SO<sub>4</sub>. Rotary evaporation of the organic material afforded 16.1 g (98%) of crude 2,3-  
46  
47 dibromopropionitrile as a golden oil. A portion of this material (470 mg, 2.2 mmol) was dissolved  
48  
49 in 7 mL of methanol along with 420 mg (4.4 mmol) of 3-hydroxypyridine in a 25 mL round-  
50  
51 bottomed flask. This mixture was heated to reflux with an oil bath for 3 h and concentrated with a  
52  
53  
54  
55  
56  
57  
58  
59  
60

1  
2  
3 rotary evaporator to give a dark brown viscous oil, which was combined with 7 mL of isopropanol  
4 and stirred vigorously at room temperature overnight. The precipitate that formed was isolated by  
5 vacuum filtration, dissolved in 2 mL of methanol, and triturated into toluene (20 mL) with stirring.  
6  
7 Vacuum filtration of the resulting solid gave 288 mg (57%) of crude **5-Br** as a brown powder.  
8  
9 Some of this material (67.2 mg, 0.290 mmol) was placed in a 6 dram vial along with 1 mL of water  
10  
11 with 210 mg (0.24 mmol) of NaBAr<sup>F</sup><sub>4</sub>. Dichloromethane (1 mL) was added and the mixture was  
12  
13 stirred overnight at room temperature. The organic fraction was subsequently washed with brine  
14  
15 (2 × 2 mL) and dried over Na<sub>2</sub>SO<sub>4</sub>. At a later date, it was triturated with hexanes until the solution  
16  
17 just became cloudy, dried over activated CaSO<sub>4</sub>, and passed through a 0.45 μm PTFE membrane.  
18  
19 Removal of the solvent under reduced pressure afforded 221 mg (91%) of a brown, slightly  
20  
21 lustrous powder (mp 157–160 °C) which was stored in a dry-box under nitrogen. <sup>1</sup>H NMR (400  
22  
23 MHz, CD<sub>2</sub>Cl<sub>2</sub>) δ 8.29 (dd, *J* = 2.0 and 1.4 Hz, 1H), 8.23 (d, *J* = 6.0 Hz, 1H), 8.17 (ddd, *J* = 9.1,  
24  
25 2.7, and 0.9 Hz, 1H), 8.04 (dd, *J* = 8.8 and 6.0 Hz, 1H), 7.87 (d, *J* = 14.4 Hz, 1H), 7.72 (s, 8H),  
26  
27 7.56 (s, 4H), 6.38 (d, *J* = 14.3 Hz, 1H). <sup>13</sup>C{<sup>1</sup>H} NMR (125 MHz, CD<sub>2</sub>Cl<sub>2</sub>) δ 162.3 (q, <sup>1</sup>*J*<sub>B-C</sub> = 62  
28  
29 Hz), 158.8, 145.5, 137.1, 135.4, 133.4, 130.6, 129.7, 129.4 (qq, <sup>2</sup>*J*<sub>F-C</sub> = 39 Hz and <sup>2</sup>*J*<sub>B-C</sub> = 3.6 Hz)  
30  
31 125.2 (q, <sup>1</sup>*J*<sub>F-C</sub> = 339 Hz), 118.1 (septet, <sup>3</sup>*J*<sub>F-C</sub> = 5.0 Hz), 112.1, 104.8. IR-ATR 3208, 1355, 1278,  
32  
33 1123 cm<sup>-1</sup>. HRMS (ESI) *m/z* [M – BAr<sup>F</sup><sub>4</sub>]<sup>+</sup> calcd for C<sub>8</sub>H<sub>7</sub>N<sub>2</sub>O 147.0553, found 147.0540.

34  
35  
36  
37  
38  
39  
40  
41  
42 ***N*-(2,4-Dinitrophenyl)-4-hydroxypyridinium BAr<sup>F</sup><sub>4</sub> (6)**. A 50 mL round-bottomed flask was  
43  
44 loaded with 200 mg (2.1 mmol) of 4-hydroxypyridine, 492 mg (2.4 mmol) of 1-chloro-2,4-  
45  
46 dinitrobenzene, and 10 mL of acetonitrile. This solution was heated to reflux with an oil bath with  
47  
48 stirring overnight, and the resulting precipitate was collected by vacuum filtration and washed with  
49  
50 acetonitrile to give 588 mg (94%) of **6-Cl** as a pale pink powder. In a 6 dram vial, 100 mg (0.336  
51  
52 mmol) of this material was dissolved in 3 mL of methanol along with 298 mg (0.336 mmol) of  
53  
54  
55  
56  
57  
58  
59  
60

1  
2  
3 NaBAR<sup>F</sup><sub>4</sub> and the mixture was stirred vigorously. After 30 min, 3 mL of CH<sub>2</sub>Cl<sub>2</sub> was added to the  
4  
5 vial and stirring continued overnight. The resulting precipitate was removed with a 0.45 μm PTFE  
6  
7 syringe filter and hexanes were added dropwise to the solution until it just became cloudy. Drying  
8  
9 with activated CaSO<sub>4</sub>, followed by a second filtration and concentration with a rotary evaporator,  
10  
11 afforded 340 mg (90%) of an off-white powder (mp 125–127 °C). <sup>1</sup>H NMR (400 MHz, CD<sub>2</sub>Cl<sub>2</sub>)  
12  
13 δ 9.27 (d, *J* = 2.5 Hz, 1H), 8.82 (dd, *J* = 8.6 and 2.5 Hz, 1H), 8.27–8.23 (m, 2H), 7.88 (d, *J* = 8.6  
14  
15 Hz, 1H), 7.72 (s, 8H), 7.56 (s, 4H), 7.50–7.46 (m, 2H). <sup>13</sup>C {<sup>1</sup>H} NMR (125 MHz, CD<sub>2</sub>Cl<sub>2</sub>) δ 174.4,  
16  
17 162.3 (q, <sup>1</sup>*J*<sub>B-C</sub> = 62 Hz), 160.0, 150.5, 145.6, 138.3, 135.4, 131.3, 131.1, 129.4 (qq, <sup>2</sup>*J*<sub>F-C</sub> = 39 Hz  
18  
19 and <sup>2</sup>*J*<sub>B-C</sub> = 3.6 Hz), 125.2 (q, <sup>1</sup>*J*<sub>F-C</sub> = 338 Hz), 123.5, 118.1 (septet, <sup>3</sup>*J*<sub>F-C</sub> = 4.7 Hz), 116.8. IR-ATR  
20  
21 3676, 3086, 1643, 1610, 1552, 1355, 1278, 1119 cm<sup>-1</sup>. HRMS (ESI) *m/z* [M – BAR<sup>F</sup><sub>4</sub>]<sup>+</sup> calcd for  
22  
23 C<sub>11</sub>H<sub>8</sub>N<sub>3</sub>O<sub>5</sub> 262.0458, found 262.0468.  
24  
25  
26  
27

28 **3-Deuterio-*N*-methylindole.**<sup>15</sup> Using CH<sub>2</sub>Cl<sub>2</sub> as an eluent, 1 mL (8.0 mmol) of *N*-methylindole  
29  
30 was passed through a small column of activated alumina. This solution was then concentrated with  
31  
32 a rotary evaporator and the resulting material was stored in a 6 dram vial under argon.  
33  
34 Concurrently, a 50 mL two-necked round-bottomed flask equipped with a reflex condenser was  
35  
36 filled with D<sub>2</sub>O (10 mL) and heated to 110 °C with an oil bath for 1 h while the system was flushed  
37  
38 with argon. The solvent was then removed via syringe and the *N*-methylindole was added along  
39  
40 with 15 mL of D<sub>2</sub>O. This mixture was heated to 80 °C with vigorous stirring under argon for 24 h,  
41  
42 then stirred for an additional 96 h at room temperature. The product was subsequently extracted  
43  
44 with CH<sub>2</sub>Cl<sub>2</sub> (1 × 15 mL) and the organic layer was dried over MgSO<sub>4</sub>. The solution was  
45  
46 concentrated in vacuo and the resulting neat liquid was passed through a plug of activated alumina  
47  
48 to give 657 mg (62%) of a pale mint green oil (99% D by <sup>1</sup>H NMR) which was stored in a glovebox  
49  
50  
51  
52  
53  
54  
55  
56  
57  
58  
59  
60

1  
2  
3 under nitrogen.  $^1\text{H}$  NMR (400 MHz,  $\text{CD}_2\text{Cl}_2$ )  $\delta$  7.60 (d,  $J = 7.9$  Hz, 1H), 7.35 (d,  $J = 8.2$  Hz, 1H),  
4 7.21 (t,  $J = 7.2$  Hz, 1H), 7.11–7.06 (m, 2H), 6.47 (d,  $J = 3.1$  Hz, 0.01 H), 3.79 (s, 3H).  
5  
6

7 **General Friedel–Crafts kinetics procedures.** To a 1 mL volumetric flask, 74.6 mg (0.500 mmol)  
8 of *trans*- $\beta$ -nitrostyrene or 70.2  $\mu\text{L}$  (87.0 mg, 0.500 mmol) of 2,2,2-trifluoroacetophenone was  
9 added along with 6.2  $\mu\text{L}$  (6.5 mg, 0.050 mmol) of *N*-methylindole and 0.005 mmol of a charged  
10 catalyst or 10  $\mu\text{L}$  of a 0.5 M solution of a non-charged catalyst in  $\text{CH}_2\text{Cl}_2$ . This mixture was diluted  
11 with  $\text{CD}_2\text{Cl}_2$  to the mark and mixed by inverting the flask twice. It was then transferred to an NMR  
12 tube which was capped and sealed with PTFE tape. The first NMR spectrum was collected within  
13 5 min of the preparation of the solvent ( $t_0$ ) and the NMR tube was maintained at 27 °C in the NMR  
14 probe (for KIE experiments) or a water bath (for all other experiments) between acquisition of  
15 subsequent spectra. When *trans*- $\beta$ -nitrostyrene was used as the electrophile, reaction progress was  
16 monitored using signals at  $\delta$  6.47 (*N*-methylindole) and  $\delta$  5.17, 5.08 and 4.98 (Friedel–Crafts  
17 product) or  $\delta$  3.79 (3-*d*-*N*-methylindole) and  $\delta$  3.74 (deuterated product) for the KIE experiments.  
18 With  $\text{PhCOCF}_3$  as the electrophile, the methyl signals at 3.79 (*N*-methylindole), 3.83 (mono  
19 addition product), and 3.74 ppm (bis addition product) were used. A pseudo-first-order kinetic  
20 model was employed to determine half-lives and rate constants (Tables S1–S4, Figures S1 and  
21 S2).  
22  
23  
24  
25  
26  
27  
28  
29  
30  
31  
32

33 **General procedure for the reaction of cyclopentadiene with methyl vinyl ketone.**  
34 Cyclopentadiene was generated by distillation from its dimer and stored at  $-78$  °C under argon for  
35 up to 3 h. Methyl vinyl ketone (MVK) was distilled within 1 week of when it was used, and was  
36 kept at 4 °C under argon. A 1 mL volumetric flask was filled with MVK (20.3  $\mu\text{L}$ , 17.5 mg, 0.250  
37 mmol), 0.0025 mmol of a charged catalyst or 10  $\mu\text{L}$  of a 0.25 M solution of a non-charged catalyst  
38 in  $\text{CH}_2\text{Cl}_2$ , and sufficient  $\text{CH}_2\text{Cl}_2$  before being mixed by inverting the stoppered flask twice. A  
39  
40  
41  
42  
43  
44  
45  
46  
47  
48  
49  
50  
51  
52  
53  
54  
55  
56  
57

1  
2  
3 portion of this solution (100  $\mu\text{L}$ ) was added to a separate 1 mL volumetric flask along with 21.0  
4  $\mu\text{L}$  (16.5 mg, 0.250 mmol) of cyclopentadiene and filled with  $\text{CD}_2\text{Cl}_2$  before mixing this mixture  
5  
6 by inverting the flask twice. This solution was then transferred to an NMR tube which was capped  
7  
8 and sealed with PTFE tape. The first NMR spectrum was collected within 5 min of solvent addition  
9  
10 ( $t_0$ ) and the NMR tube was maintained at 25  $^\circ\text{C}$  in the NMR probe between acquisition of  
11  
12 subsequent spectra. Reaction progress was monitored using signals at 2.24 (MVK), 2.08 (*endo*),  
13  
14 and 2.17 ppm (*exo*) (Table S5, Figure S3). A pseudo-first-order kinetic model was used to  
15  
16 determine half-lives and rate constants.  
17  
18  
19  
20

21 **Solution IR procedure.** A 6 dram vial was loaded with **3** (29.2 mg, 25.6  $\mu\text{mol}$ ),  $\text{CCl}_4$  (5 mL), and  
22  
23  $\text{CD}_3\text{CN}$  (50  $\mu\text{L}$ ) and this mixture was stirred until all of the catalyst dissolved. A separate solution  
24  
25 of 5 mL of  $\text{CCl}_4$  and 50  $\mu\text{L}$  of  $\text{CD}_3\text{CN}$  with no catalyst was also prepared and a background  
26  
27 spectrum of this mixture was recorded in a 10 mm liquid cell that was stored in a dry-box under  
28  
29 nitrogen. This cell was subsequently emptied and purged with nitrogen for 1 min before being  
30  
31 reloaded with the sample solution. A new spectrum was obtained and background corrected.  
32  
33  
34

35 **General procedure for UV-vis titrations.** 7-Methyl-2-phenylimidazo[1,2-*a*]pyrazin-3(*7H*)-one  
36  
37 (**7**), was kept under vacuum (0.05–0.1 torr) for at least 12 h before use. Three volumetric flasks  
38  
39 were employed to prepare the required solutions as follows: A 1 mL volumetric flask was filled  
40  
41 with 1.0–1.5 mg (4.4–6.7  $\mu\text{mol}$ ) of **7** and sufficient  $\text{CH}_2\text{Cl}_2$  to afford solution A. In a 5 mL  
42  
43 volumetric flask, 25  $\mu\text{L}$  of solution A was diluted with  $\text{CH}_2\text{Cl}_2$  to the line to give solution B. A  
44  
45 separate 5 mL volumetric flask was used to prepare solution C, which consisted of 25  $\mu\text{L}$  of  
46  
47 solution A, 25–30 molar equivalents of catalyst relative to **7**, and sufficient  $\text{CH}_2\text{Cl}_2$  to fill the flask  
48  
49 to the line. Background UV-vis spectra of  $\text{CH}_2\text{Cl}_2$  from 300–950 nm were collected before each  
50  
51 sample spectrum in a 10 mm quartz cuvette with a screw-on PTFE septum cap. For the titrations,  
52  
53  
54  
55  
56  
57  
58  
59  
60

1  
2  
3 2 mL of solution B were placed in a separate cuvette and the UV-vis spectrum was recorded.  
4  
5 Subsequently, 10  $\mu\text{L}$  of solution C was added via syringe and the solution was swirled for 15 s and  
6  
7 a new spectrum was obtained. Further mixing of the solution for an additional 10 s was carried out  
8  
9 and the spectrum was re-recorded. This was repeated, if necessary, until consecutive spectra  
10  
11 differed by no more than 1 nm in  $\lambda_{\text{max}}$  and 0.010 absorbance units. Additional aliquots of solution  
12  
13 C were added and the spectra were recorded in the same way until  $\lambda_{\text{max}}$  did not change over three  
14  
15 consecutive additions (**1**, **2**, **4**, and **5**) or until at least 20 molar equivalents of catalyst relative to  
16  
17 the **7** had been added (**6**). Equilibrium binding constants ( $K$ ) were determined using absorbance  
18  
19 values at 440, 470, 500, and 530 nm by carrying out non-linear fits of the resulting binding  
20  
21 isotherms using the Supramolecular BindFit app ([app.supramolecular.org/bindfit](http://app.supramolecular.org/bindfit)).<sup>21</sup> In each case,  
22  
23 1:1, 2:1, and 1:2 associations were explored, though all of the data are in accord with 1:1 binding  
24  
25 except for the results with **6**, which are consistent with 1:2 binding (Table S6). While  $\lambda_{\text{max}}$  for the  
26  
27 1:1 complex can be obtained directly in the former instances, it cannot in the latter case.  
28  
29 Consequently,  $\lambda_{\text{max}(1:1)}$  was determined by plotting  $\chi_{1:1}/\lambda_{\text{max}}$  versus  $\chi_{1:1}$ , where  $\chi_{1:1}$  is the mole  
30  
31 fraction of the 1:1 complex as obtained from the BindFit output file.<sup>22</sup> The reciprocal of the sum  
32  
33 of the slope and y-intercept from the resulting linear least squares fit afforded  $\lambda_{\text{max}(1:1)}$ . These values  
34  
35 are all within 1.0 nm of the directly-observed, leveled-off determinations with **1**, **2**, **4**, and **5**.  
36  
37  
38  
39  
40

41  
42 **Catalyst titration procedures with triethylphosphine oxide.** Triethylphosphine oxide was  
43  
44 stored and weighed in a glovebox under nitrogen. For the titration with **1**, 2.1–2.4 mg (15.7–17.9  
45  
46  $\mu\text{mol}$ ) of  $\text{Et}_3\text{PO}$  was dissolved in minimal  $\text{CH}_2\text{Cl}_2$ , transferred to a 1 mL volumetric flask, and  
47  
48 diluted to the mark (solution A). In a separate 1 mL volumetric flask, **1** (9.4–10.0 mg,  
49  
50 9.7–10.3  $\mu\text{mol}$ ) was added and diluted to the line with  $\text{CH}_2\text{Cl}_2$  (solution B). An NMR tube was  
51  
52 then filled with 100  $\mu\text{L}$  of solution A and 400  $\mu\text{L}$  of  $\text{CD}_2\text{Cl}_2$ . An initial NMR spectrum was  
53  
54  
55  
56  
57

1  
2  
3 obtained to establish the  $^{31}\text{P}$  chemical shift of  $\text{Et}_3\text{PO}$ . Subsequently, 80  $\mu\text{L}$  of solution B was added  
4  
5 via microsyringe to the NMR tube, which was then inverted twice before obtaining another  
6  
7 spectrum. This process was repeated until the  $^{31}\text{P}$  signal shifted by no more than 0.1 ppm in three  
8  
9 consecutive spectra (Table S7, Figure S15). For the other catalysts, full titrations were not carried  
10  
11 out. In these cases, 5.0 mg (37.3  $\mu\text{mol}$ ) of  $\text{Et}_3\text{PO}$  were placed in a 1 mL volumetric flask which  
12  
13 was filled to the line with  $\text{CH}_2\text{Cl}_2$ . An NMR tube was loaded with 135  $\mu\text{L}$  of this solution and 315  
14  
15  $\mu\text{L}$  of  $\text{CD}_2\text{Cl}_2$  to obtain the initial  $^{31}\text{P}$  NMR signal of  $\text{Et}_3\text{PO}$ . Subsequently, 7.5  $\mu\text{mol}$  of the selected  
16  
17 catalyst and 500  $\mu\text{L}$  of  $\text{CH}_2\text{Cl}_2$  were added with mixing and a second  $^{31}\text{P}$  NMR spectrum was  
18  
19 recorded to obtain the change in the chemical shift.  
20  
21  
22

23  
24 **Computations.** Calculations were performed at the Minnesota Supercomputing Institute using  
25  
26 Gaussian 16<sup>23</sup> with the B3LYP functional and the 6-31G+(d,p) basis set.<sup>24</sup> Full geometry  
27  
28 optimizations and subsequent vibrational frequency determinations were carried out and all of the  
29  
30 given stationary points correspond to energy minima with no negative eigenvalues (Table S8).  
31  
32 Unscaled vibrational frequencies were used to obtain zero-point energies, thermal corrections to  
33  
34 the enthalpies at 298 K, and entropies. Low frequency modes that contribute more than  $\frac{1}{2}\text{RT}$  to  
35  
36 the enthalpy correction were replaced with  $\frac{1}{2}\text{RT}$ .  
37  
38  
39  
40  
41

42 **Supporting Information Available:** Kinetic, UV-vis titration, and  $\text{Ph}_3\text{PO}$   $^{31}\text{P}$  chemical shift data  
43  
44 are provided along with plots of  $\ln k_{\text{Diels-Alder}}$  vs  $\ln K_{1:1}$  and  $\Delta G^\circ_{\text{acid}}$ , NMR spectra, computed  
45  
46 structures and energies, the complete citation to ref. 23, and a reference. This material is available  
47  
48 free of charge via the internet at <http://pubs.acs.org>.  
49  
50

## 51 AUTHOR INFORMATION

### 52 Corresponding Author

53  
54  
55  
56 \*E-mail: [kass@umn.edu](mailto:kass@umn.edu).  
57

1  
2  
3 **ORCID**  
4

5 Steven R. Kass: 0000-0001-7007-9322  
6

7 **Notes**  
8

9 The authors declare no competing financial interests.  
10  
11  
12

13 **ACKNOWLEDGMENT**  
14

15 Generous support from the National Science Foundation (CHE-1665392) and the Minnesota  
16  
17 Supercomputing Institute for Advanced Computational Research are gratefully acknowledged.  
18  
19  
20  
21  
22  
23  
24  
25  
26  
27  
28  
29  
30  
31  
32  
33  
34  
35  
36  
37  
38  
39  
40  
41  
42  
43  
44  
45  
46  
47  
48  
49  
50  
51  
52  
53  
54  
55  
56  
57  
58  
59  
60

## REFERENCES

- (1) (a) Akiyama, T. Stronger Brønsted Acids. *Chem. Rev.* **2007**, *107*, 5744-5758. (b) Akiyama, T.; Mori, K. Stronger Brønsted Acids: Recent Progress. *Chem. Rev.* **2015**, *115*, 9277-9306.
- (2) (a) Schreiner, P. R. Metal-Free Organocatalysis Through Explicit Hydrogen Bonding Interactions. *Chem. Soc. Rev.* **2003**, *32*, 289-296. (b) Doyle, A. G.; Jacobsen, E. N. Small-Molecule H-Bond Donors in Asymmetric Catalysis. *Chem. Rev.* **2007**, *107*, 5713-5743. (c) Giacalone, F.; Gruttadauria, M.; Agrigento, P.; Noto, R. Low-Loading Asymmetric Organocatalysis. *Chem. Soc. Rev.* **2012**, *41*, 2406-2447. (d) Phipps, R. J.; Hamilton, G. L.; Toste, F. D. The Progression of Chiral Anions From Concepts to Applications in Asymmetric Catalysis. *Nature Chemistry* **2012**, *4*, 603-614. (e) Wende, R. C.; Schreiner, P. R. Evolution of Asymmetric Organocatalysis: Multi- and Retrocatalysis. *Green Chem.* **2012**, *14*, 1821-1849. (f) Auvil, T. J.; Schafer, A. G.; Mattson, A. E. Design Strategies for Enhanced Hydrogen-Bond Donor Catalysts. *Eur. J. Org. Chem.* **2014**, 2633-2646.
- (3) (a) Akiyama, T.; Itoh, J.; Yokota, K.; Fuchibe, K. Enantioselective Mannich-Type Reaction Catalyzed by A Chiral Brønsted Acid. *Angew. Chem. Int. Ed.* **2004**, *43*, 1566-1568. (b) Akiyama, T.; Morita, H.; Itoh, J.; Fuchibe, K. Chiral Brønsted Acid Catalyzed Enantioselective Hydrophosphonylation of Imines: Asymmetric Synthesis of Alpha-Amino Phosphonates. *Org. Lett.* **2005**, *7*, 2583-2585. (c) Lippert, K. M.; Hof, K.; Gerbig, D.; Ley, D.; Hausmann, H.; Guenther, S.; Schreiner, P. R. Hydrogen-Bonding Thiourea Organocatalysts: The Privileged 3,5-Bis(trifluoromethyl)phenyl Group. *Eur. J. Org. Chem.* **2012**, 5919-5927. (d) Zhang, Z.; Bao, Z.; Xing, H. N,N'-Bis[3,5-bis(trifluoromethyl)phenyl]thiourea: A Privileged Motif for Catalyst Development. *Org. Biomol. Chem.* **2014**, *12*, 3151-3162. (e) Yao, Y.; Shu, H.; Tang, B.; Chen, S.; Lu, Z.; Xue, W. Synthesis, Characterization and Application of Some Axially Chiral Binaphthyl

1  
2  
3 Phosphoric Acids in Asymmetric Mannich Reaction. *Chim. J. Chem.* **2015**, *33*, 601-609. (f) Zhou,  
4 F. T.; Yamamoto, H. A Powerful Chiral Phosphoric Acid Catalyst for Enantioselective  
5 Mukaiyama-Mannich Reactions. *Angew. Chem. Int. Ed.* **2016**, *55*, 8970-8974.  
6  
7

8  
9  
10 (4) (a) Jensen, K. H.; Sigman, M. S. Systematically Probing the Effect of Catalyst Acidity in a  
11 Hydrogen-Bond-Catalyzed Enantioselective Reaction. *Angew. Chem. Int. Ed.* **2007**, *46*, 4748-  
12 4750. (b) Jensen, K. H.; Sigman, M. S. Evaluation of Catalyst Acidity and Substrate Electronic  
13 Effects in a Hydrogen Bond-Catalyzed Enantioselective Reaction. *J. Org. Chem.* **2010**, *75*, 7194-  
14 7201. (c) Li, X.; Deng, H.; Zhang, B.; Li, J.; Zhang, L.; Luo, S.; Cheng, J.-P. Physical Organic  
15 Study of Structure–Activity–Enantioselectivity Relationships in Asymmetric Bifunctional  
16 Thiourea Catalysis: Hints for the Design of New Organocatalysts. *Chem. Eur. J.* **2010**, *16*, 450-  
17 455. (d) Kaupmees, K.; Tolstoluzhsky, N.; Raja, S.; Rueping, M.; Leito, I. On the Acidity and  
18 Reactivity of Highly Effective Chiral Brønsted Acid Catalysts: Establishment of an Acidity Scale.  
19 *Angew. Chem. Int. Ed.* **2013**, *52*, 11569-11572.  
20  
21

22  
23  
24 (5) (a) Samet, M.; Buhle, J.; Zhou, Y.; Kass, S. R. Charge-Enhanced Acidity and Catalyst  
25 Activation. *J. Am. Chem. Soc.* **2015**, *137*, 4678-4680. (b) Fan, Y.; Kass, S. R. Electrostatically  
26 Enhanced Thioureas. *Org. Lett.* **2016**, *18*, 188-191. (c) Ma, J.; Kass, S. R. Electrostatically  
27 Enhanced Phosphoric Acids: A Tool in Brønsted Acid Catalysis. *Org. Lett.* **2016**, *18*, 5812-5815.  
28 (d) Payne, C.; Kass, S. R. Structural Considerations for Charge-Enhanced Brønsted Acid Catalysts.  
29 *J. Phys. Org. Chem.* **2020**, *33*, xxx-yyy (DOI: 10.1002/poc.4069).  
30  
31

32  
33  
34 (6) Jung, M. E.; Buszek, K. R. The Stereochemistry of Addition of Trialkylammonium and  
35 Pyridinium Tetrafluoroborate Salts to Activated Acetylenes. Preparation of Novel Dienophiles for  
36 Diels–Alder Reactions. *J. Am. Chem. Soc.* **1988**, *110*, 3965-3969.  
37  
38

39  
40  
41 (7) Katritzky, A. R.; Rahimi-Rastgoo, S.; Sabongi, G. J.; Fischer, G. W. 1,3-Dipolar Character of  
42  
43  
44  
45  
46  
47  
48  
49  
50  
51  
52  
53  
54  
55  
56  
57  
58  
59  
60

1  
2  
3 Six-Membered Aromatic Rings. Part 51. Cycloadditions of 1-( $\beta$ -Benzoylvinyl)-3-Oxidopyri-  
4 diniums and Subsequent Transformations. *J. Chem. Soc., Perkin Trans. 1* **1980**, 362-371.

5  
6  
7  
8 (8) Eicher-Lorka, O.; Kupetis, G. K.; Rastenyté, L.; Matijo, A. A Convenient Preparation of 1-  
9 Vinylpyridinium Salts. *Synthesis* **1999**, *12*, 2131-2137.

10  
11  
12 (9) Eda, M.; Kurth, M. J.; Nantz, M. H. The Solid-Phase Zincke Reaction: Preparation of  $\omega$ -  
13 Hydroxy Pyridinium Salts in the Search for CFTR Activation. *J. Org. Chem.* **2000**, *65*, 5131-5135.

14  
15  
16  
17 (10) (a) Huynh, P. N. H.; Walvoord, R. R.; Kozlowski, M. C. Rapid Quantification of the  
18 Activating Effects of Hydrogen-Bonding Catalysts with a Colorimetric Sensor. *J. Am. Chem. Soc.*  
19 **2012**, *134*, 15621-15623. (b) Walvoord, R. R.; Huynh, P. N. H.; Kozlowski, M. C. Quantification  
20 of Electrophilic Activation by Hydrogen-Bonding Organocatalysts. *J. Am. Chem. Soc.* **2014**, *136*,  
21 16055-16065.

22  
23  
24 (11) The  $\lambda_{\max}$  values are not as good a measure of catalyst acidity or activity.

25  
26  
27 (12) Diemoz, K. M.; Franz, A. K. NMR Quantification of Hydrogen-Bond-Activating Effects for  
28 Organocatalysts Including Boronic Acids. *J. Org. Chem.* **2019**, *84*, 1126-1138.

29  
30  
31 (13) (a) Herrera, R. P.; Sgarzani, V.; Bernard, L.; Ricci, A. Catalytic Enantioselective Friedel-  
32 Crafts Alkylation of Indoles with Nitroalkenes by Using a Simple Thiourea Organocatalyst.  
33 *Angew. Chem. Int. Ed.* **2005**, *44*, 6576-6579. (b) Ganesh, M.; Seidel, D. Catalytic Enantioselective  
34 Additions of Indoles to Nitroalkenes. *J. Am. Chem. Soc.* **2008**, *130*, 16464-16465. (c) Itoh, J.;  
35 Fuchibe, K.; Akiyama, T. Chiral Phosphoric Acid Catalyzed Enantioselective Friedel-Crafts  
36 Alkylation of Indoles with Nitroalkenes: Cooperative Effect of 3 Angstrom Molecular Sieves.  
37 *Angew. Chem., Int. Ed.* **2008**, *47*, 4016-4018. (d) Hermeke, J.; Toy, P. H. Phosphonium Ion Tagged  
38 Chiral Phosphoric Acids and Their Application in Friedel-Crafts Reactions of Indoles.  
39 *Tetrahedron* **2011**, *67*, 4103-4109. (e) Marqués-López, E.; Alcaine, A.; Tejero, T.; Herrera, R. P.

Enhanced Efficiency of Thiourea Catalysts by External Brønsted Acids in the Friedel–Crafts Alkylation of Indoles. *Eur. J. Org. Chem.* **2011**, 3700-3705. (f) Shokri, A.; Wang, X.-B.; Kass, S. R. Electron-Withdrawing Trifluoromethyl Groups in Combination with Hydrogen Bonds in Polyols: Brønsted Acids, Hydrogen-Bond Catalysts, and Anion Receptors. *J. Am. Chem. Soc.* **2013**, *135*, 9525-9530.

(14) (a) Cooper, J. D.; Vitullo, V. P.; Whalen, D. L. Evidence for a Change in Rate-Determining Step of the Acid-Catalyzed Hydrolysis of a Vinyl Ether. *J. Am. Chem. Soc.* **1971**, *93*, 6294-6296.

(b) Sayer, J. M.; Jencks, W. P. Mechanism and Catalysis of 2-Methyl-3-thiosemicarbazone Formation. A Second Change in Rate-Determining Step and Evidence for a Stepwise Mechanism for Proton Transfer in a Simple Carbonyl Addition Reaction. *J. Am. Chem. Soc.* **1973**, *95*, 5637-5649. (c) Okuyama, T.; Komoguchi, S.; Fueno, T. Reaction of Thiols with Phenylglyoxal to Give Thioesters of Mandelic Acid. 2. Intramolecular General-Base Catalysis and Change in Rate-Determining Step. *J. Am. Chem. Soc.* **1982**, *104*, 2582-2587. (d) Jiang, Y.-Y.; Liu, T.-T.; Zhang, R.-X.; Xu, Z.-Y.; Sun, X.; Bi, S. Mechanism and Rate-Determining Factors of Amide Bond Formation through Acyl Transfer of Mixed Carboxylic–Carbamic Anhydrides: A Computational Study. *J. Org. Chem.* **2018**, *83*, 2676-2685.

(15) This compound previously was reported and a similar procedure was employed. For further details, see: Wang, S.; Nie, J.; Zheng, Y.; Ma, J.-A. A Direct Copper-Promoted Three-Component Entry to Trifluoromethylketoximes. *Org. Lett.* **2014**, *16*, 1606-1609.

(16) (a) Wang, Y.; Yuan, Y.; Xing, C.-H.; Lu, L. Trifluoromethanesulfonic Acid-Catalyzed Solvent-Free Bisindolylolation of Trifluoromethyl Ketones. *Tetrahedron Lett.* **2014**, *55*, 1045-1048.

(b) Liu, X.-D.; Wang, Y.; Ma, H.-Y.; Xing, C.-H.; Yuan, Y.; Lu, L. Cs<sub>2</sub>CO<sub>3</sub>-Catalyzed Alkylation of Indoles with Trifluoromethyl Ketones. *Tetrahedron* **2017**, *73*, 2283-2289. (c) Ma, J.; Kass, S.

R. Asymmetric Arylation of 2,2,2-Trifluoroacetophenones Catalyzed by Chiral Electrostatically-Enhanced Phosphoric Acids. *Org. Lett.* **2018**, *20*, 2689-2692.

(17) This also applies to the Friedel–Crafts reaction rate constants.

(18) Unfortunately, we were unable to measure the corresponding quantity for triflic acid as the solution became opaque when 1 equivalent of TfOH was added to a  $1.0 \times 10^{-6}$  M solution of **7** in  $\text{CH}_2\text{Cl}_2$ .

(19) Harris, R. K.; Becker, E. D.; Cabral de Menezes, S. M.; Goodfellow, R.; Granger, P. NMR Nomenclature. Nuclear Spin Properties and Conventions for Chemical Shifts. *Pure Appl. Chem.* **2001**, *73*, 1795-1818.

(20) Miura, K.; Sugimoto, J.; Oshima, K.; Utimoto, K. Triethylborane Induced Radical Reaction of Ketene Silyl Acetals with Polyhalomethanes. *Bull. Chem. Soc. Jpn.* **1992**, *65*, 1513-1521.

(21) (a) Thordarson, P. Determining Association Constants From Titration Experiments in Supramolecular Chemistry. *Chem. Soc. Rev.* **2011**, *40*, 1305-1323. (b) Hibbert, B. D.; Thordarson, P. The Death of the Job Plot, Transparency, Open Science and Online Tools, Uncertainty Estimation Methods and Other Developments in Supramolecular Chemistry Data Analysis. *Chem. Commun.* **2016**, *52*, 12792-12805. (c) Also, see: [supramolecular.org](http://supramolecular.org).

(22) For additional details, see ref. 5d.

(23) Frisch, M. J.; Trucks, G. W.; Schlegel, H. B.; Scuseria, G. E.; Robb, M. A., et al., Gaussian 16; Gaussian, Inc., Wallingford CT, 2016.

(24) (a) Becke, A. D. Density-Functional Thermochemistry. III. The Role of Exact Exchange. *J. Chem. Phys.* **1993**, *98*, 5648-5652. (b) Lee, C.; Yang, W.; Parr, R. G. Development of the Colle-Salvetti Correlation-Energy Formula into a Functional of the Electron Density. *Phys. Rev. B* **1988**, *37*, 785–789.

## Table of Content Graphic

